# Single-shot high-resolution identification of discrete frequency modes of single-photon-level optical pulses

Daisuke Yoshida [1,2,*] Mayuka Ichihara,[1] Takeshi Kondo,[1] Feng-Lei Hong,[1] and Tomoyuki Horikiri[1]

[1]*Yokohama National University, 79-5 Tokiwadai, Hodogaya, Yokohama 240-8501, Japan*
[2]*LQUOM, Inc., 79-5 Tokiwadai, Hodogaya, Yokohama 240-8501, Japan*

Frequency-multiplexed quantum communication usually requires a single-shot identification of the frequency mode of a single photon. In this paper, we propose a scheme that can identify the frequency mode with high resolution even for spontaneously emitted photons whose generation time is unknown, by combining the time-to-space and frequency-to-time mode mapping. We also demonstrate the mapping of the frequency mode (100 MHz intervals) to the temporal mode (435 ns intervals) for weak coherent pulses using atomic frequency combs. This frequency interval is close to the minimum frequency mode interval of the atomic frequency comb quantum memory with the $Pr^{3+}$-ion-doped $Y_2SiO_5$ crystal, and the proposed scheme has the potential to maximize the frequency multiplexing of the quantum repeater scheme with the memory.

## I. INTRODUCTION

The realization of quantum communication enables various applications such as quantum key distribution [1,2], blind quantum computing [3], and atomic clocks with unprecedented stability and accuracy [4]. Quantum repeaters enable long distance quantum communication and are expected to constitute the core technology for the future quantum internet [5]. For these reasons, extensive studies have been conducted in recent years toward their realization. One trend is frequency multiplexing which is necessary for improving the entanglement distribution rate for quantum communication [6,7]. In frequency-multiplexed quantum communication, the identification of frequency modes is usually necessary. The frequency mode identification of single photons used in quantum communication is more difficult than that of classical light, mainly because it must be measured in a single shot, unless nondestructive measurement of the photon is possible.

Recently, an impactful study on quantum repeaters was reported by Lago-Rivera *et al.* [8]. The authors demonstrated a quantum repeater scheme [9] that combines time-division multiplexed absorptive quantum memories based on an atomic frequency comb (AFC) scheme [10] and photon-pair sources. The AFC is a comb-shaped absorption profile. It can be used not only as a time-multiplexing but also as a frequency-multiplexing memory [6,11,12]. Here, we consider frequency multiplexing of the quantum repeater scheme [8,9]. In this case, AFCs are required to store photons of multiple frequency modes, and photon sources are required to generate photon pairs of frequency modes corresponding to those of AFCs. In Ref. [8], the AFC was tailored in inhomogeneous broadening of the $^3H_4 \leftrightarrow {}^1D_2$ transition in the $Pr^{3+}$-ion-doped $Y_2SiO_5$ crystal (Pr:YSO) by the hole-burning technique [13].

In the case of the AFC in Pr:YSO, the upper bandwidth limit of one frequency mode is about 4 MHz and the lower limit of the interval between frequency modes is about 100 MHz when used as a memory capable of reading out stored photons on demand [14]. These limits are determined by the hyperfine level spacing in Pr:YSO [14]. The region where AFCs are created is limited to within the inhomogeneous broadening of Pr:YSO. Therefore, in the case of a frequency-multiplexed quantum repeater using AFCs in Pr:YSO, the upper limit of the entanglement distribution rate can be increased by making the frequency mode interval as narrow as possible. As a frequency-multiplexed photon pair source, cavity-enhanced spontaneous parametric down-conversion (cSPDC) [15–17], which is also used in Ref. [8], would be promising. The frequency mode interval of the photons generated by cSPDC depends on the free spectral range (FSR) of the cavity. In Ref. [8], where entanglement between quantum memories was generated by single-photon interference, the pump laser for cSPDC was continuous wave (cw). In the case of cw excitation, the time at which photon pairs are generated is unknown. To summarize the above, for frequency multiplexing of the quantum repeater scheme performed in Ref. [8], a method to identify high-resolution frequency modes of narrow linewidth photons without photon generation time information is desired.

A frequency-to-time mode mapper (FTMM) [18–21] and a frequency-to-space mode mapper (FSMM) [22,23] allow frequency mode identification of single photons. Typical examples of FTMMs are wavelength dispersion [20] and chirped fiber Bragg gratings [21]. In general, these are superior in that they are easy to implement but face difficulties in achieving resolution below GHz. An FTMM using AFCs is also possible [18,19]. In this method, the resolution is determined by the homogeneous broadening width and the energy level spacing used, and currently, high resolution below GHz has been achieved [19]. However, the FTMM that can be adapted

---
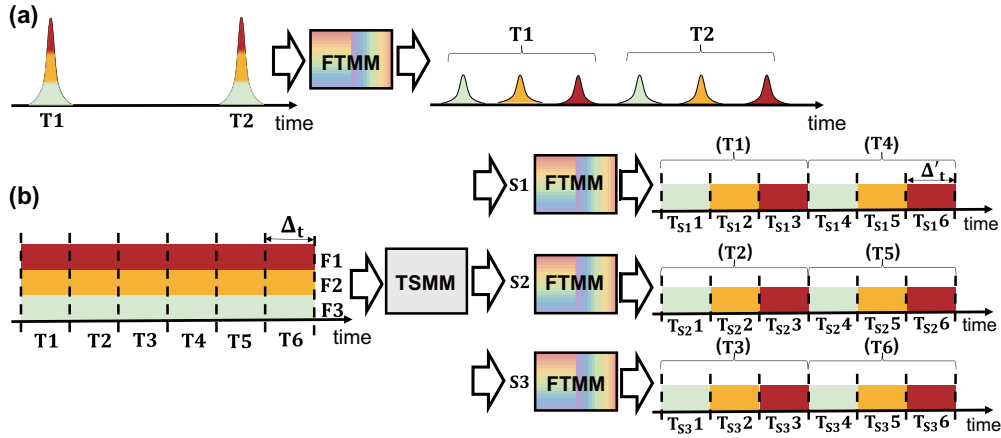
FIG. 1. (a) Schematic of mapping frequency mode to temporal mode. (b) Diagram of frequency mode identification combining a TSMM and FTMMs. Temporal modes T1 and T4 are mapped to spatial mode S1, temporal modes T2 and T4 are mapped to spatial mode S2, and temporal modes T3 and T6 are mapped to spatial mode S3 using a TSMM. The frequency mode is then mapped to the temporal mode by an FTMM, which is provided for each spatial mode. From the combination of spatial and temporal modes after mapping, the frequency mode can be uniquely determined.

to photons with narrow linewidths below 10 MHz has not been realized. A common drawback of FTMMs is that they require information about the generation time of the photon for which the frequency mode is to be identified. In contrast, an FSMM can identify the frequency mode without information about the photon generation time since frequency is identified by spatial mode. However, in general it is not easy to achieve a high resolution of less than GHz.

In this paper, we propose a scheme that can identify high-resolution frequency modes of narrow-linewidth photons without photon generation time information by combining a time-to-space mode mapper (TSMM) and FTMMs. We also demonstrate a high-resolution FTMM using AFCs, which can be applied to narrow-linewidth photons. The demonstrated FTMM is capable of identifying frequency modes in the 100 MHz interval, which is close to the FSR of recent cSPDC two-photon sources [8,17] and the lower limit of the frequency interval of AFCs in Pr:YSO.

## II. SCHEME

In this section, we initially propose a frequency mode identification scheme that combines FTMMs and a TSMM. Next, we describe FTMMs using AFCs.

### A. Frequency mode identification

First, we consider frequency mode identification when only an FTMM is used. A schematic diagram of this case is shown in Fig. 1(a). By mapping multiple frequency modes, which exist in the same temporal mode, it is possible to identify the frequency mode from the observation time of the photon if its generation time is known. In this case, however, to prevent multiple frequency modes from existing in the same temporal mode after frequency-to-time mode mapping, the number of temporal modes before mapping must be reduced. From the view of the communication rate, reducing the number of temporal modes is a disadvantage. Therefore, we propose

a frequency mode identification scheme combining FTMMs and a TSMM. In this scheme, frequency modes can be identified even if the photon generation time is unknown. It also eliminates the need to reduce the number of temporal modes before FTMMs and a TSMM. The overview diagram is shown in Fig. 1(b). Consider the case where the generation time of the photon is unknown; i.e., the probability of the photon's existence is equally present at all times. The duration of the temporal mode of the input photon is set to be $\Delta_t$. Here, $\Delta_t$ is assumed to be sufficiently longer than the coherence time of the photon. The TSMM converts each temporal mode separated by $\Delta_t$ into spatial modes $S_1, S_2, \ldots, S_{N_S}, S_1, \ldots$ with $N_S$ being the total number of spatial modes. The FTMM provided for each spatial mode converts each frequency mode to a temporal mode at $\Delta'_t$ intervals. At this time, $\Delta_t \leqq \Delta'_t$ must be satisfied to ensure that different frequency modes do not exist in the same temporal mode. For the same reason, if the total number of frequency modes is $N_F$, it must satisfy $N_F \Delta'_t \leqq N_S \Delta_t$. In this way, the frequency mode can be uniquely determined from the spatial and temporal modes in which the photon was observed. Figure 1(b) shows the case $\Delta_t = \Delta'_t$, $N_F = N_S = 3$. The frequency resolution of this scheme depends on the resolution of the FTMMs. A promising candidate for a high-resolution FTMM is the AFC, which we describe below. A promising candidate for the TSMM could be an optical switch array using electro-optic modulators (EOMs) [24].

### B. A frequency-to-time mode mapper using an atomic frequency comb

The AFC is an equally spaced comb-shaped absorption profile as shown in Fig. 2(a). Photons absorbed in the AFC are reemitted in the same spatial mode in the inverse time of the comb spacing $\Delta$ (henceforth referred to as the echo signal). Typically, AFCs are created by hole-burning in inhomogeneous broadening of rare-earth-ion-doped crystals. The AFC can also read out the absorbed photons on
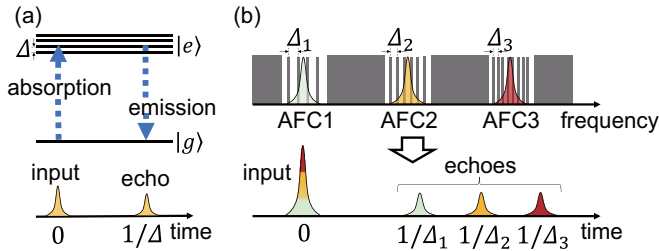
FIG. 2. (a) Schematic diagram representing the function of AFC. The light pulse absorbed at time 0 is reemitted at time $1/\Delta$. (b) Schematic diagram of B with AFCs. AFCs with different comb spacing, $\Delta_1$, $\Delta_2$, $\Delta_3$, are made for each frequency mode to be identified. The light pulses are reemitted in different temporal modes for each frequency mode.

demand by using another ground level with no population [10,25,26]. In this study, frequency-to-time mode mapping was performed by AFC, which is used as a fixed-time memory.

AFC is considered to be used as a high-resolution FTMM. A schematic diagram of frequency-to-time mode mapping using AFC is shown in Fig. 2(b). Multiple AFCs can be tailored in inhomogeneous broadening [6,11,12]. If AFCs are tailored with different comb intervals for each frequency mode, the time at which the echoes are reproduced can be changed for each frequency mode. However, it is not possible to create multiple AFCs in arbitrary bands because creating a hole in one band will create antiholes in other bands. The lower limit of the interval between frequency modes is about 100 MHz when used as a memory capable of reading out stored photons on demand [14]. The spacing between adjacent AFCs should be at least 100 MHz [14]. Therefore in this study, experiments were conducted to map three frequency modes separated by $\sim$100 MHz into temporal modes with $\Delta_t' \sim 435$ ns spacing.

## III. EXPERIMENTAL SETUP

The overall experiment setup is illustrated in Fig. 3. In our experiment, multiple AFCs were created within inhomogeneous broadening of Pr:YSO which had a $Pr^{3+}$ doping rate
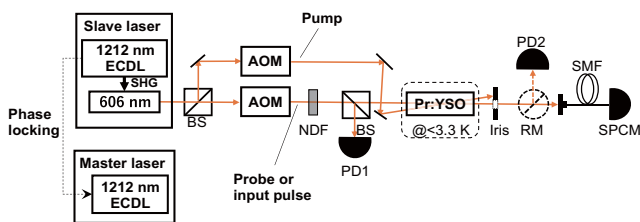


FIG. 3. Experimental setup. Second harmonic generation (SHG) of 1212 nm external cavity diode laser (ECDL) is used as pump, probe, and input pulses. A neutral density filter (NDF) is used to reduce the input pulse to a single-photon level. The input pulse is coupled to a single-mode fiber and observed by an SPCM. When observing AFCs, the NDF is removed and the transmitted light was observed with a photodetector (PD1) instead of an SPCM. The other photodetector (PD2) is used to monitor the probe laser intensity. BS, beamsplitter; RM, removal mirror mount.

of 0.05% and dimensions of 3 mm $\times$ 3 mm $\times$ 5 mm. A wide modulation range is required for the laser beam to create an AFC in multiple frequency modes by taking advantage of the inhomogeneous broadening of Pr:YSO (about 10 GHz [13]). In this study, we developed a frequency stabilization and modulation system that can perform accurate GHz-order modulation using a dynamical phase lock technique [27] and accurate and fast modulation of approximately 10 MHz using an acousto-optic modulator (AOM) [28]. The absolute frequency of the master laser (Toptica, TA pro) was stabilized to an optical frequency comb phase-locked to the GPS signals and the linewidth was narrowed using a reference cavity. The slave laser (Toptica, TA-SHG pro) used for pump, probe, and input pulses was stabilized against the master laser. We used a closed-cycle cryostat (Montana Instruments, Cryostation) to cool the Pr:YSO crystal to $<$3.3 K. Each AFC was created by modulating the pump laser by 10 MHz using the AOM in the double-path configuration [28]. After each AFC is created, the laser itself is modulated by 100 MHz using the dynamic phase lock technique, and a different AFC was created by modulation with the AOM again. The time required for 100 MHz modulation was approximately 10 ms in our setup. In this way, three AFCs with different comb spacing were created at 100 MHz intervals.

The probe laser for observing the created AFC can be turned on and off by an AOM. It was turned off during AFC creation and turned on only during observation. During AFC observation, the probe laser was modulated by chirping the reference rf signal for phase locking in the dynamical phase lock technique [27]. The input pulse for observing the echo signal of the AFC was the same path as the probe laser. The input pulse was tailored by the AOM to be Gaussian with full width at half maximum (FWHM) of 5 MHz. The echo signal is coupled to a single mode fiber (SMF) and detected by a single-photon counting module (SPCM; Perkin Elmer, SPCM-AQRH-14-FC). The coupling efficiency of the SMF was 59%, the detection efficiency of the SPCM was 59%, and the dark count rate is $\sim$150 Hz. The power of the pump laser was set to $\sim$2.6 mW, the probe laser to 1 μW, and the input pulse to mean photon number $\mu = 0.12$ per pulse. The beam diameter was set to $\sim$500 μm for the pump and $\sim$100 μm for the probe and input pulses. These polarizations were aligned with the D2 axis of the Pr:YSO crystal.

## IV. EXPERIMENTAL RESULT

The three AFCs were observed by chirping a weak probe laser at a chirp rate of 5.2 MHz/ms. The optical depth shown in Fig. 4 was the average of 16 measurements. It can be seen that AFCs with different comb spacings were created. In this experiment, the comb spacing was set to $\Delta_1 = 1.533$ MHz, $\Delta_2 = 920$ kHz, and $\Delta_3 = 657$ kHz, respectively, in order from the low-frequency side. This means that the expected echo times are $t_1 = 652$ ns, $t_2 = 1087$ ns, and $t_3 = 1522$ ns.

In this experiment, for each frequency mode created with multiple frequency modes, 10 000 Gaussian pulses were input. By repeating this procedure, the total number of pulses input for each frequency mode was $N_{in} = 7.5 \times 10^5$. The observed results are shown in Fig. 5. It can be seen that the echoes appear in the expected temporal mode for each
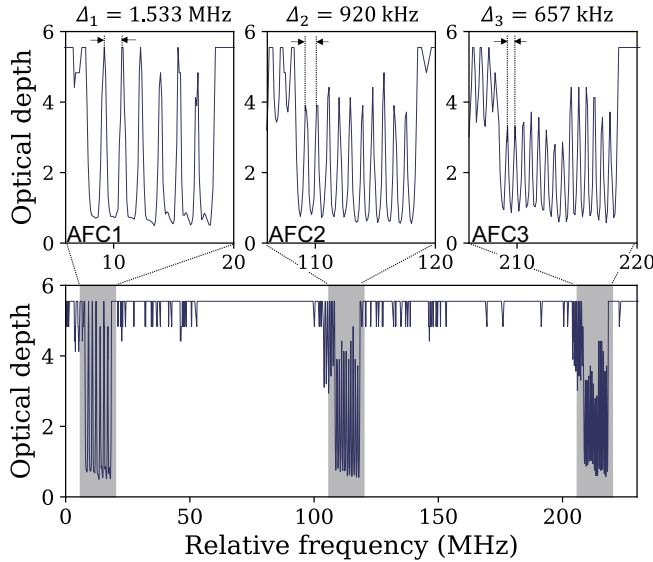
FIG. 4. An overall view of the three AFCs and an enlarged view of each AFC.

frequency mode. Table I shows the expected temporal mode of detection for each frequency mode, echo efficiency $\eta_{\text{echo}}$, and probability $\eta_{\text{error}}$ of observing a photon in the other two expected temporal modes. $\eta_{\text{echo}}$ is the ratio of the number of counts within the expected temporal mode (corrected for SPCM detection efficiency and fiber coupling loss) to the total number of photons input ($N_{\text{in}}\mu$). $\eta_{\text{error}}$ is the ratio of the number of counts within the other two temporal modes that are not expected (corrected for SPCM detection efficiency and fiber coupling loss) to $N_{\text{in}}\mu$.

## V. DISCUSSION

In this study, three frequency modes at 100 MHz intervals were successfully mapped in different temporal modes.
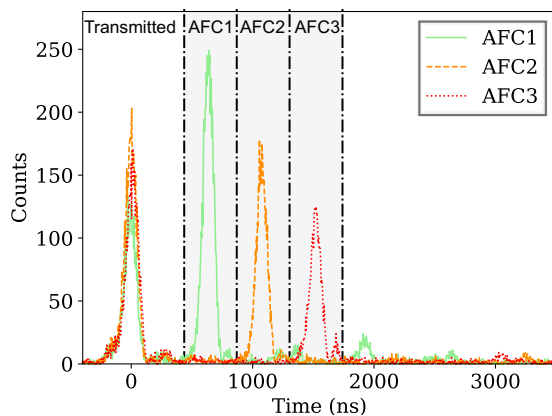


FIG. 5. Echo signal observation results. The bin size is 4.096 ns. The gray shaded area surrounded by dashed-dotted black lines is the temporal mode in which each echo is expected to appear. The second echo caused by reabsorption of the echo signal was also observed, and the third echo caused by AFC3 was sufficiently small and was considered negligible.

TABLE I. Comb spacing and temporal mode for each AFC, and experimental results for $\eta_{\text{echo}}$ and $\eta_{\text{error}}$. Time window for each temporal mode is 435 ns.

|  | AFC1 | AFC2 | AFC3 |
| --- | --- | --- | --- |
| $\Delta$ | 1.533 MHz | 920 kHz | 657 kHz |
| Temporal mode | 652 ns | 1087 ns | 1522 ns |
| $\eta_{\text{echo}}$ | 21% | 14% | 11% |
| $\eta_{\text{error}}$ | 2.2% | 1.4% | 1.2% |

However, the probability of successful mapping is low, about 10%. Moreover, since the absorption efficiency of AFC is not unit, the photons that are transmitted without being absorbed exist around 0 ns in Fig. 5 and occupy the temporal mode. Theoretically, near unit efficiency absorption and reemission can be obtained by using an AFC in a cavity [29], which would help in resolving these problems.

We consider the limits of the number of frequency modes for an FTMM using AFCs. Factors that determine the limit include the modulation range of the pump laser, inhomogeneous broadening, linewidth of the pump laser, and the creation time of the AFC. In our system, the laser was directly modulated, but the modulation range is limited by the mode-hop range, which is about 15 GHz. Alternatively, the inhomogeneous width of the Pr:YSO doping rate of 0.05% that we used is 10 GHz [13]. Therefore, if we were to create an AFC with different comb spacing every 100 MHz, the limit would be about 100 modes. In fact, if we assume a time width of 435 ns for one temporal mode and try to create an AFC with different comb spacing in 100 modes, the comb spacing of the AFC with the smallest comb spacing will be 20 kHz, and the linewidth of the pump laser must be sufficiently narrowed. In the current system, the lower limit of the comb spacing that can be stably produced is about 500 kHz, and to achieve even smaller comb spacing, it is necessary to use an ultralow expansion cavity or self-heterodyne method for narrowing the linewidth of the pump laser [30,31]. The upper limit of the allowable AFC creation time is determined by the relaxation time between hyperfine levels, since the comb structure degrades after the AFC is created. In this experiment, the time to create one AFC was <50 ms and the time for frequency mode modulation was ~10 ms. Therefore, the time required to create an $N$ mode AFC is <60$N$ ms. The extent to which the creation time is acceptable will depend on the system to which the AFC is applied.

This scheme is expected to be applied not only to multiplexing for quantum communication but also to various spectroscopic measurements. However, when AFC is used as an FTMM, frequency conversion is required to perform frequency mode identification of photons in various frequency bands. Coupling of AFC in Pr:YSO with telecommunication wavelength photons using frequency conversion has been achieved [32,33]. In contrast, an FSMM using a virtually imaged phased array (VIPA) [23] or gratings [22] is also expected as a frequency mode identification method. Compared to our scheme, they are superior in terms of ease of implementation and frequency band extension. The superiority of our scheme is that it allows for high-resolution frequency identification.

## VI. CONCLUSION

In this study, we achieved frequency mode identification at 100 MHz intervals, which is close to the frequency multiplexing limit of AFC in Pr:YSO, a promising quantum memory for quantum repeaters. Since the FSR of a cSPDC source with high coupling to quantum memory has been demonstrated to be about 100 MHz [8,17], this spectroscopic system not only achieves the upper limit of discrete mode spectral resolution with Pr:YSO, but also shows promising results for improving the quantum entanglement generation rate.

[1] C. H. Bennett, G. Brassard, and J.-M. Robert, Privacy amplification by public discussion, SIAM J. Comput. **17**, 210 (1988).

[2] C. H. Bennett, G. Brassard, and N. D. Mermin, Quantum Cryptography without Bell's Theorem, Phys. Rev. Lett. **68**, 557 (1992).

[3] A. Broadbent, J. Fitzsimons, and E. Kashefi, Universal blind quantum computation, in *Proceedings of the 50th Annual IEEE Symposium on Foundations of Computer Science* (IEEE Computer Society, Los Alamitos, CA, 2009), pp. 517–526.

[4] P. Kómár, E. M. Kessler, M. Bishof, L. Jiang, A. S. Sørensen, J. Ye, and M. D. Lukin, A quantum network of clocks, Nat. Phys. **10**, 582 (2014).

[5] H. J. Kimble, The quantum internet, Nature (London) **453**, 1023 (2008).

[6] N. Sinclair, E. Saglamyurek, H. Mallahzadeh, J. A. Slater, M. George, R. Ricken, M. P. Hedges, D. Oblak, C. Simon, W. Sohler, and W. Tittel, Spectral Multiplexing for Scalable Quantum Photonics using an Atomic Frequency Comb Quantum Memory and Feed-Forward Control, Phys. Rev. Lett. **113**, 053603 (2014).

[7] S. Wengerowsky, S. K. Joshi, F. Steinlechner, H. Hübel, and R. Ursin, An entanglement-based wavelength-multiplexed quantum communication network, Nature (London) **564**, 225 (2018).

[8] D. Lago-Rivera, S. Grandi, J. V. Rakonjac, A. Seri, and H. de Riedmatten, Telecom-heralded entanglement between multimode solid-state quantum memories, Nature (London) **594**, 37 (2021).

[9] C. Simon, H. de Riedmatten, M. Afzelius, N. Sangouard, H. Zbinden, and N. Gisin, Quantum Repeaters with Photon Pair Sources and Multimode Memories, Phys. Rev. Lett. **98**, 190503 (2007).

[10] M. Afzelius, C. Simon, H. de Riedmatten, and N. Gisin, Multimode memory based on atomic frequency combs, Phys. Rev. A **79**, 052329 (2009).

[11] A. Seri, D. Lago-Rivera, A. Lenhard, G. Corrielli, R. Osellame, M. Mazzera, and H. de Riedmatten, Quantum Storage of Frequency-Multiplexed Heralded Single Photons, Phys. Rev. Lett. **123**, 080502 (2019).

[12] T.-S. Yang, Z.-Q. Zhou, Y.-L. Hua, X. Liu, Z.-F. Li, P.-Y. Li, Y. Ma, C. Liu, P.-J. Liang, X. Li, Y.-X. Xiao, J. Hu, C.-F. Li, and G.-C. Guo, Multiplexed storage and real-time manipulation based on a multiple degree-of-freedom quantum memory, Nat. Commun. **9**, 3407 (2018).

[13] M. Nilsson, L. Rippe, S. Kröll, R. Klieber, and D. Suter, Hole-burning techniques for isolation and study of individual hyperfine transitions in inhomogeneously broadened solids demonstrated in $Pr^{3+}$: $Y_2SiO_5$, Phys. Rev. B **70**, 214116 (2004).

[14] A. Ortu, J. V. Rakonjac, A. Holzäpfel, A. Seri, S. Grandi, M. Mazzera, H. de Riedmatten, and M. Afzelius, Multimode capacity of atomic-frequency comb quantum memories, Quantum Sci. Technol. **7**, 035024 (2022).

[15] Z. Y. Ou and Y. J. Lu, Cavity Enhanced Spontaneous Parametric Down-Conversion for the Prolongation of Correlation Time between Conjugate Photons, Phys. Rev. Lett. **83**, 2556 (1999).

[16] D. Rieländer, A. Lenhard, M. Mazzera, and H. de Riedmatten, Cavity enhanced telecom heralded single photons for spin-wave solid state quantum memories, New J. Phys. **18**, 123013 (2016).

[17] K. Niizeki, D. Yoshida, K. Ito, I. Nakamura, N. Takei, K. Okamura, M.-Y. Zheng, X.-P. Xie, and T. Horikiri, Two-photon comb with wavelength conversion and 20-km distribution for quantum communication, Commun. Phys. **3**, 138 (2020).

[18] E. Saglamyurek, M. Grimau Puigibert, Q. Zhou, L. Giner, F. Marsili, V. B. Verma, S. Woo Nam, L. Oesterling, D. Nippa, D. Oblak, and W. Tittel, A multiplexed light-matter interface for fibre-based quantum networks, Nat. Commun. **7**, 11202 (2016).

[19] E. Saglamyurek, N. Sinclair, J. A. Slater, K. Heshami, D. Oblak, and W. Tittel, An integrated processor for photonic quantum states using a broadband light-matter interface, New J. Phys. **16**, 065019 (2014).

[20] M. Avenhaus, A. Eckstein, P. J. Mosley, and C. Silberhorn, Fiber-assisted single-photon spectrograph, Opt. Lett. **34**, 2873 (2009).

[21] A. O. C. Davis, P. M. Saulnier, M. Karpiński, and B. J. Smith, Pulsed single-photon spectrometer by frequency-to-time mapping using chirped fiber Bragg gratings, Opt. Express **25**, 12804 (2017).

[22] R. Cheng, C.-L. Zou, X. Guo, S. Wang, X. Han, and H. X. Tang, Broadband on-chip single-photon spectrometer, Nat. Commun. **10**, 4104 (2019).

[23] O. Pietx-Casas, G. C. do Amaral, T. Chakraborty, R. Berrevoets, T. Middelburg, J. A. Slater, and W. Tittel, Spectrally multiplexed Hong-Ou-Mandel interference, arXiv:2111.13610.

[24] X. Tu, C. Song, T. Huang, Z. Chen, and H. Fu, State of the art and perspectives on silicon photonic switches, Micromachines **10**, 51 (2019).

[25] M. Afzelius, I. Usmani, A. Amari, B. Lauritzen, A. Walther, C. Simon, N. Sangouard, J. Minář, H. de Riedmatten, N. Gisin, and S. Kröll, Demonstration of Atomic Frequency Comb Memory for Light with Spin-Wave Storage, Phys. Rev. Lett. **104**, 040503 (2010).

[26] N. Timoney, I. Usmani, P. Jobez, M. Afzelius, and N. Gisin, Single-photon-level optical storage in a solid-state spin-wave memory, Phys. Rev. A **88**, 022324 (2013).

[27] K. Numata, J. R. Chen, and S. T. Wu, Precision and fast wavelength tuning of a dynamically phase-locked widely-tunable laser, Opt. Express **20**, 14234 (2012).

[28] E. A. Donley, T. P. Heavner, F. Levi, M. O. Tataw, and S. R. Jefferts, Double-pass acousto-optic modulator system, Rev. Sci. Instrum. **76**, 063112 (2005).

[29] M. Afzelius and C. Simon, Impedance-matched cavity quantum memory, Phys. Rev. A **82**, 022310 (2010).

[30] B. C. Young, F. C. Cruz, W. M. Itano, and J. C. Bergquist, Visible Lasers with Subhertz Linewidths, Phys. Rev. Lett. **82**, 3799 (1999).

[31] F. Kéfélian, H. Jiang, P. Lemonde, and G. Santarelli, Ultralow-frequency-noise stabilization of a laser by locking to an optical fiber-delay line, Opt. Lett. **34**, 914 (2009).

[32] N. Maring, K. Kutluer, J. Cohen, M. Cristiani, M. Mazzera, P. M. Ledingham, and H. de Riedmatten, Storage of up-converted telecom photons in a doped crystal, New J. Phys. **16**, 113021 (2014).

[33] K. Mannami, T. Kondo, T. Tsuno, T. Miyashita, D. Yoshida, K. Ito, K. Niizeki, I. Nakamura, F.-L. Hong, and T. Horikiri, Coupling of a quantum memory and telecommunication wavelength photons for high-rate entanglement distribution in quantum repeaters, Opt. Express **29**, 41522 (2021).